

## Inelastic design of high-axially loaded concrete columns in moderate seismicity regions

Johnny Ching Ming Ho

*Department of Civil Engineering, The University of Hong Kong, Pokfulam Road, Hong Kong, P.R.C.*

*(Received November 16, 2010, Accepted May 25, 2011)*

**Abstract.** In regions of high seismic risk, high-strength concrete (HSC) columns of tall buildings are designed to be fully ductile during earthquake attack by providing substantial amount of confining steel within the critical region. However, in areas of low to moderate seismic risk, the same provision of confining steel is too conservative because of the reduced seismic demand. More critically, it causes problematic steel congestion in the beam-column joints and column critical region. This will eventually affect the quality of concrete placing owing to blockage. To relieve the problem, the confining steel in the critical region of HSC columns located in low to moderate seismicity regions can be suitably reduced, while maintaining a limited ductility level. Despite the advantage, there are still no guidelines developed for designing limited ductility HSC columns. In this paper, a formula for designing limited ductility HSC columns is presented. The validity of the formula was verified by testing half-scale HSC columns subjected to combined high-axial load and flexure, in which the confining steel was provided as per the proposed formula. From the test results, it is evident that the curvature ductility factors obtained for all these columns were about 10, which is the generally accepted level of limited ductility.

**Keywords:** axial load; columns; confinement; flexural strength; high-strength concrete; limited ductility; reinforced concrete

---

### 1. Introduction

Recently, with the advent of ultra-fine materials such as micro-silica and slags, as well as the super-plasticiser for workability enhancement, there is rapid development of the technology in producing high-strength concrete (HSC). Nowadays, HSC with concrete strength of 100 MPa is readily available in the industry for construction of columns in tall building structures. Because of its higher strength-to-weight ratio, it is particularly popular in the column construction of high-rise buildings. Apart from having higher strength, HSC also has larger elastic modulus, shear strength and tensile strength (Logan *et al.* 2009, Kwan 2000). However, since HSC is more brittle than normal-strength concrete (NSC) in compression, the design of HSC columns should be treated differently from that of NSC columns. Furthermore, the larger elastic modulus of HSC causes less dilation of concrete core during axial compression and thereby reducing the confining pressure produced by the confining (or transverse) steel in columns (Mirmiran and Shahawy 1997, Lu and

---

\*Corresponding author, Assistant Professor, E-mail: [johnny.ho@hku.hk](mailto:johnny.ho@hku.hk)

Hsu 2007). The situation is even worse for HSC columns subjected to combined high-axial load and flexure. Because of the reduced confining effect, high-axially loaded HSC columns may fail in a very brittle manner in extreme events such as impact, blasting and earthquake (Inel *et al.* 2008, Weerheijm *et al.* 2009, Yagob *et al.* 2009).

For buildings located in regions of moderate seismic risk, the design of reinforced concrete (RC) structures should consider appropriate methods of dissipating the enormous energy induced by earthquake attack. This can be generally achieved by installing dampers (Chen and Ding 2008, Ghosh and Ghosh 2008, Li and Xiong 2008, Chung *et al.* 2009, Fu 2009, Kavianipour and Sadati 2009, Wu and Cai 2009), adopting base isolation design (Hino *et al.* 2008, Kim *et al.* 2008a, 2008b, Ates *et al.* 2009) or by improving the confining pressure provided to the concrete core such that the column is ductile enough to form plastic hinges at designated location(s). The structures are then able to dissipate excessive energy through inelastic structural damage but not collapse (Lu and Zhou 2007, Bindhu *et al.* 2008, Bechtoula *et al.* 2009, Zhang *et al.* 2009, Sadjadi and Kianoush 2010). The first two methods are popular in tall and special buildings, while the last method is more suitable in low and medium rise buildings because of the ease of installation and cost effectiveness. In this design approach, the plastic hinge region of columns, which is designed to be at the base of the first storey column for developing a beam-sidesway mechanism (Park 2001), is normally heavily confined. This can be achieved by: (1) installing confining (or transverse) steel with close spacing and/or in larger diameter (Park 1982, Li *et al.* 1991, Ho and Pam 2003a), (2) confining the concrete member using circular or rectangular hollow steel tube (Ellobody and Young 2006, Bambach *et al.* 2008, Feng and Young 2009), (3) using external steel plate (Altin *et al.* 2008, Su *et al.* 2009, Zhu and Su 2010), (4) wrapping the concrete member by fibre reinforced polymer (Hashemi *et al.* 2008, Wu and Wei 2010). Amongst these methods, the first one of installing sufficient confining steel is the simplest and is mostly adopted in practical construction of columns in building structures.

Various research was conducted previously regarding the flexural strength and ductility performance of RC columns confined with different amount of confining steel. It has been reported experimentally (Li *et al.* 1991, Bayrak and Sheikh 1998, Paultre *et al.* 2001, Ho and Pam 2003b) and theoretically (Wu *et al.* 2004, Elemenshawi and Brown 2009, Kaklauskas *et al.* 2009, Lam *et al.* 2009a) by different researchers that HSC columns were extremely brittle if they were not confined adequately. Furthermore, for the same ductility performance, the confining steel provided to HSC columns should be significantly more than that provided to NSC columns because of the reduced concrete core dilation effect (Pam and Ho 2001, Lam *et al.* 2009b, Ho *et al.* 2010). Hence, it is evident that, in addition to designing adequate flexural strength for high-axially loaded HSC columns, they should also be designed to contain sufficient confining steel to provide ductility to the columns. Accordingly, a complete review of the design of HSC columns using performance-based approach (Lew 2007, Englekirk 2008) is necessary.

For RC moment-resisting framed buildings located in high seismic risk regions, the plastic hinges are usually designed to form at the base of the first storey columns, which are subjected to very high axial load due to gravity loadings on upper storeys. These high-axially loaded columns are usually designed to be fully ductile (Watson and Park 1994, Bayrak and Sheikh 1998, Paultre *et al.* 2001), which means that large amount of confining steel should be provided in the critical regions for plastic hinge formation (Pam and Ho 2009, Yan and Au 2010) and moment redistribution (Maghsoudi and Bengar 2006, Chen *et al.* 2009) during earthquake attack. However, in regions of low to moderate seismicity, where the structures are subjected to reduced ductility demand (Tsang *et*

*al.* 2009), this will increase the construction cost and, most importantly, causes unnecessary steel congestion in the proximity of the beam-column joint. This will also cause wastage of steel and unnecessarily increase the embodied energy or carbon level in the structures. To resolve this problem, the amount of confining steel may be suitably reduced while maintaining a moderate level of flexural ductility. Till date, many of the reported experimental research on HSC columns are to investigate the flexural ductility performance of fully ductile columns containing congested confining steel (Park 1982, Li *et al.* 1991, Sheikh *et al.* 1994, Watson and Park 1994, Bayrak and Sheikh 1998, Paultre *et al.* 2001, Bae and Bayrak 2008), whereas, tests on the flexural ductility behaviour of limited ductility HSC columns are very limited.

In this paper, five HSC columns, three of them (NEW specimens) designed as per the author's previously proposed equation for limited ductility HSC columns (Ho 2011), and two of them (BS specimens) designed as per ultimate shear resistance requirement of the former British Standard BS8110, were fabricated and tested under combined high axial load level and large reverse inelastic displacement. The columns were made of cylinder strength up to 85 MPa and the axial load level is set at 0.6 of the axial capacity of the columns. The ductility performance of these columns was assessed by the ultimate displacement and curvature ductility factors. From the test results, it was observed that the NEW specimens performed much better in terms of flexural strength and ductility than the BS specimens. More importantly, all NEW specimens can achieve a curvature ductility factors of about 10, which is considered adequate for the design of limited ductility HSC columns (Watson *et al.* 1994).

## 2. Experimental programme

Five specimens (3 NEW and 2 BS specimens) were fabricated and tested in a 6600 kN self-reaction steel-loading frame under combined compressive axial load and cyclic inelastic displacement excursions. The concrete compressive cylinder strength of the specimens varied from 50 to 85 MPa. The compressive axial load level and longitudinal steel ratio were kept constant at 0.6 of axial load capacity of column and 6.1% respectively. This is because for column subjected to

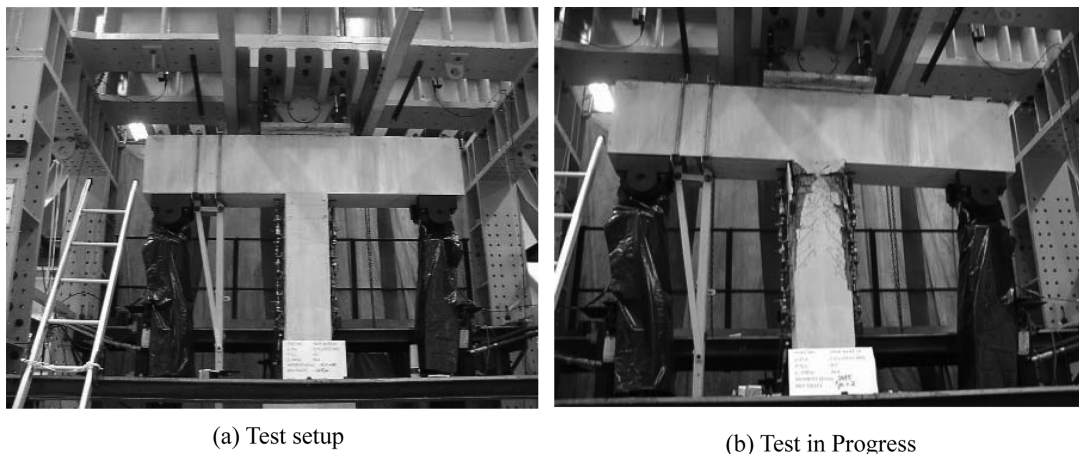


Fig. 1 Test set-up

Table 1 Details of column test specimens

Unit code	$f'_c$ (MPa)	Average $P/A_g f'_c$	Longitudinal steel		Transverse steel within potential plastic hinge region		
			Content	$\rho$ (%)	$d$ (mm)	$s$ (mm)	$\rho_s$ (%)
NEW-60-06-61-S	50.0	0.61	8T32	6.1	T12	70	2.10
NEW-60-06-61-C	56.1	0.59	8T32	6.1	T12	110	2.00
NEW-100-06-61-C	85.0	0.64	8T32	6.1	T16	120	3.20
BS-60-06-61-S	51.1	0.60	8T32	6.1	R6	100	0.38
BS-60-06-61-C	53.2	0.60	8T32	6.1	R8	210	0.47

Note: R = Mild steel round bar ( $f_y = 250$  MPa)

T = High yield deformed bar ( $f_y = 460$  MPa)

BS - Confining steel designed as per ultimate shear resistance of former BS 8110

NEW - Confining steel designed complying with Eq. (1)

very large axial load level (usually for the lower storey columns), the percentage of longitudinal steel is usually very large so that the size of the column can be minimised to save extra floor area. Moreover, the ductility of concrete columns subjected to high axial load is not sensitive to the ratio of longitudinal steel because the steel would normally not yield at ultimate state (Ho *et al.* 2010). Thus, in this study, the maximum longitudinal steel ratio allowed by Eurocode (EC2 2004) of 6% was adopted in all test specimens. The confining steel yield strength is 531 MPa. The reversed cyclic bending moment and displacement were applied by bending the column end via a horizontal rigid beam, which was cast monolithically with the column. Fig. 1 shows the test setup and during the test process. Table 1 summarises the details of the column test specimens.

## 2.1 Test specimens

Fig. 2 shows the loading application and a typical test specimen consisting of a column, a horizontal rigid beam and a top flange. Fig. 3 shows the details of cross-section of all specimens. The cross-section dimensions are 325 mm  $\times$  325 mm and the height is 1515 mm. It represents a real column in an RC moment-resisting framed building between the contra-flexure (at about mid-height) and the maximum bending moment points (at beam-column interface). The confining steel content within critical region was calculated using Eq. (1) (Ho 2010), while that outside the critical region was designed as per the shear resistance. This is to demonstrate the effective of confining reinforcement in enhancing the ductility of HSC columns.

$$\rho_s = 1.02 \left( \frac{A_g}{A_c} \right) \left( 0.2 - 0.16 \frac{\rho f_y}{f'_c} \right) \left( \frac{P}{A_g f'_c} \right)^{0.9} \left( \frac{f'_c}{f_{ys}} \right) + 0.008 \quad (1)$$

The confining steel provided according to Eq. (1) shall have its ends bent by at least 135° to form a 45° hook with a minimum continuation length of  $6d_s$  from the tangent point, where  $d_s$  is the diameter of confining steel (Fig. 3). The 135° hooks within critical regions will provide effective lateral restraint to the longitudinal steel from inelastic buckling even after the concrete cover had spalled off. The validity of the equation for limited ductility HSC columns is verified through testing high-axially loaded half-scale HSC columns subjected to flexure in this study. The critical

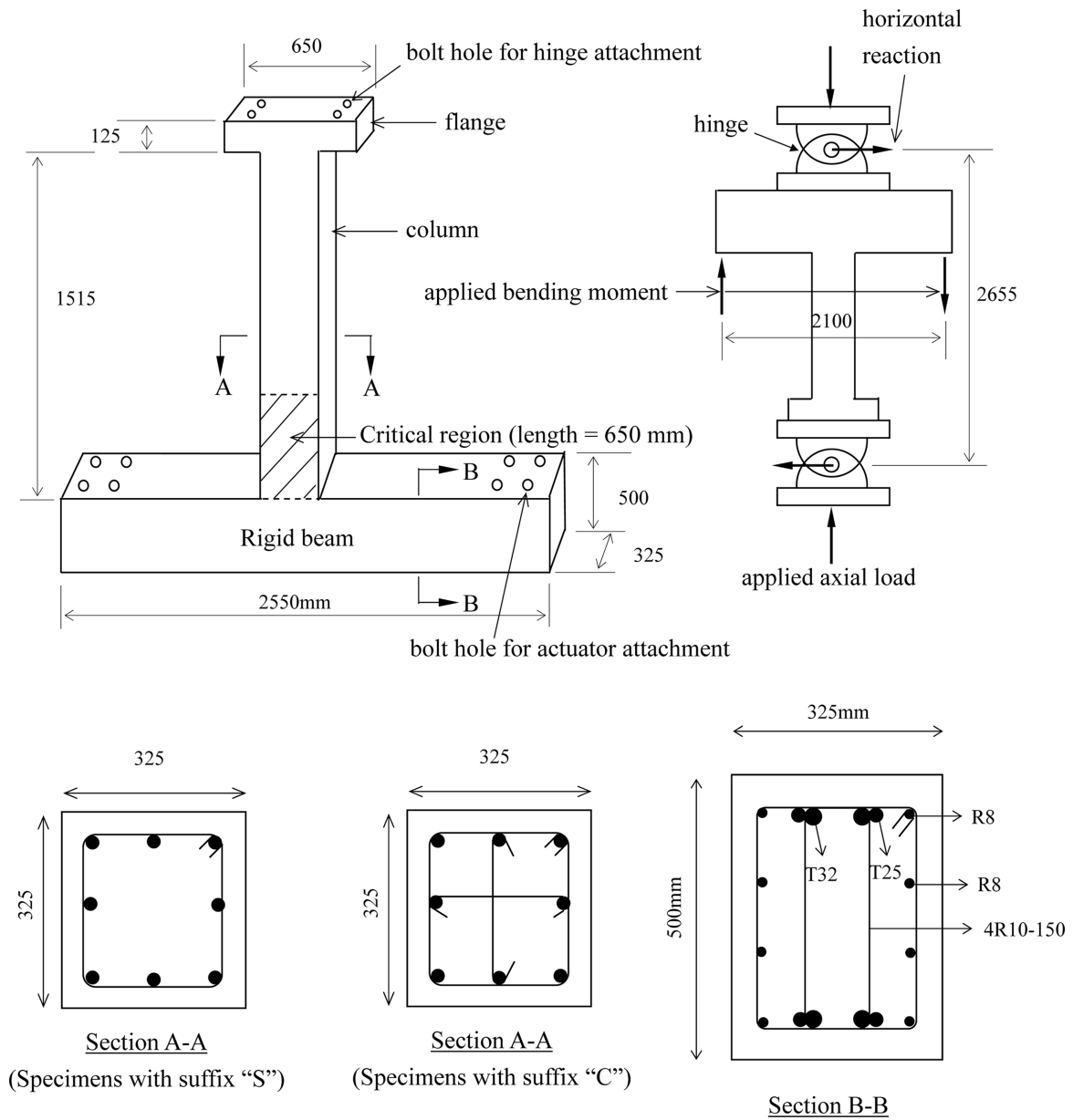


Fig. 2 Perspective view and loading application of the test specimens

region of 650 mm (from the beam-column interface) was adopted for all specimens. The applicability of the proposed critical region length will also be verified in the test.

The horizontal rigid beam was designed to behave elastically throughout the test and provide fixed support to one of the column ends, where the maximum moment occurred. The flange at the other end of the column was designed sufficiently strong to resist the flexure and shear in order to facilitate attachment of the hinge of the loading frame.

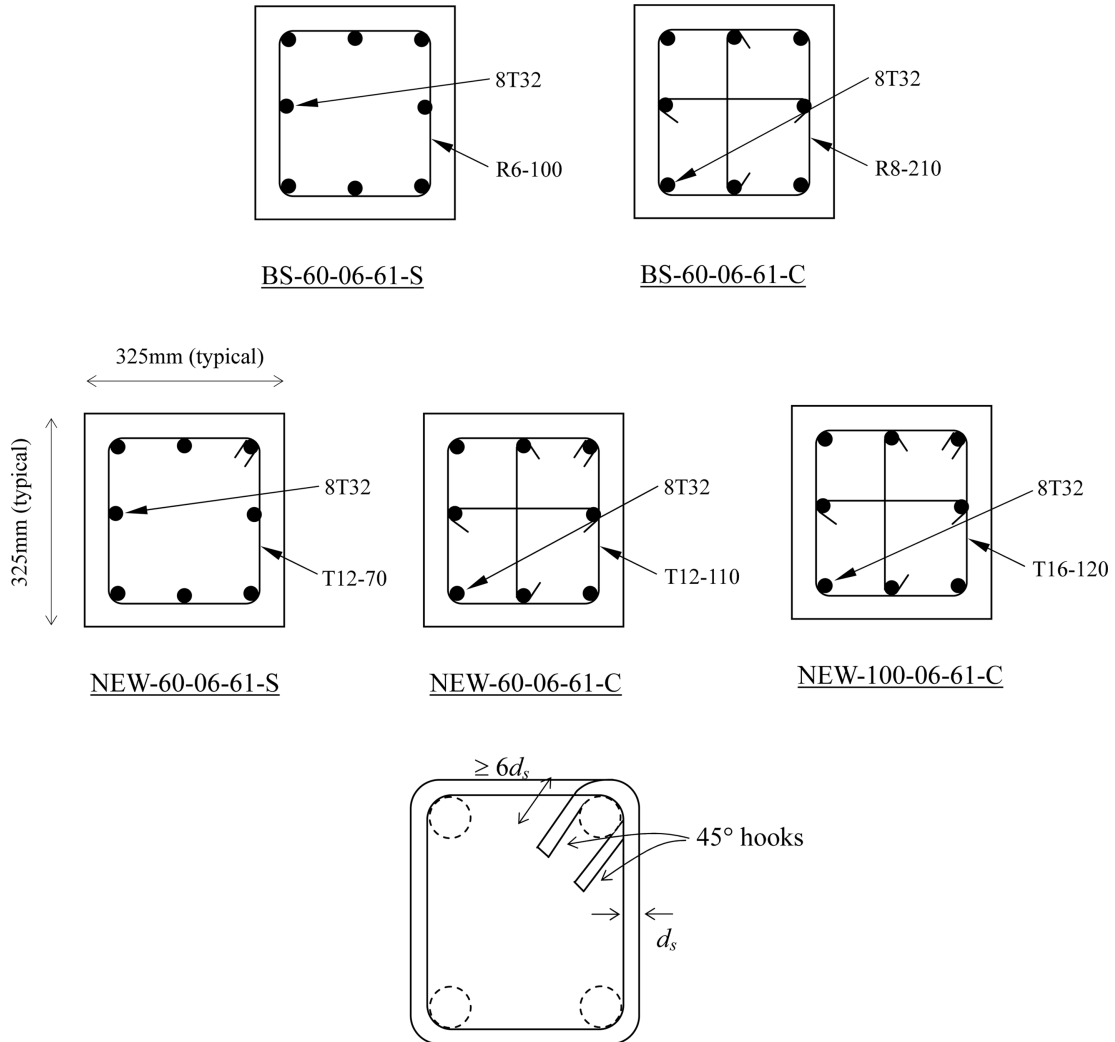
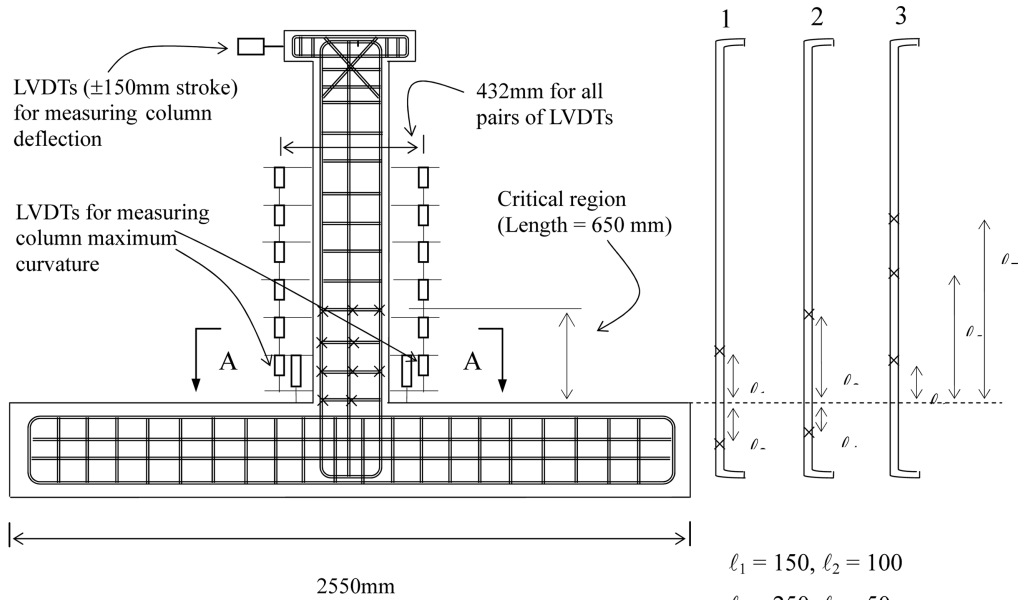


Fig. 3 Details of cross section and hooks of confining steel within critical region

## 2.2 Instrumentation

Strain gauges were attached on both longitudinal and confining steel to measure the bending and shear or confining strains respectively. Seven pairs of Linear Variable Displacement Transducer (LVDTs) were installed on the extreme tension and compression fibres of the test specimens. The reading obtained by the pair of LVDTs located at 25 mm above the beam-column interface was used to evaluate the maximum column curvature. A  $\pm 150$  mm stroke LVDT was installed at the column tip to measure the lateral deflections (drifts). There were built-in load cells in the MTS actuators to measure the applied load. An external load cell was installed on the hydraulic actuator to measure the applied axial load. The locations of strain gauges and LVDTs are shown in Fig. 4.

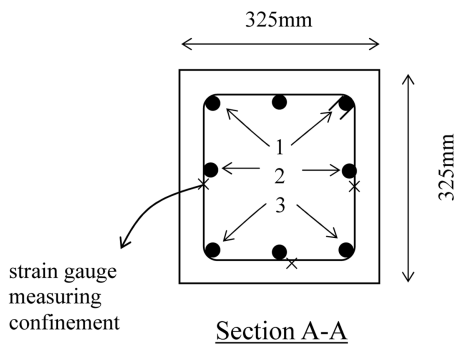


(a) LVDTs on column and strain gauges on confining steel

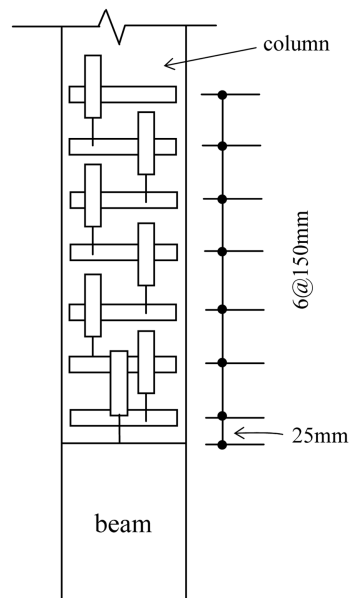
(Note: Anchorage length of longitudinal steel into rigid beam is 32 bar diameter.)

$l_1 = 150, l_2 = 100$   
 $l_3 = 250, l_4 = 50$   
 $l_5 = 400, l_6 = 75 \text{ \& } l_7 = 600$   
 (Unit: mm)

(b) Strain gauges on main bar



(c) Strain gauges on confining steel



(d) LVDTs (stroke  $\pm 25\text{mm}$  or  $\pm 50\text{mm}$ ) on extreme fibre of column face

Fig. 4 Details of instrumentation

### 2.3 Test procedure

The first cycle was load-controlled, in which the column was loaded to subsequently  $0.75 M_u$  and  $-0.75 M_u$ , where positive indicates clockwise direction and  $M_u$  is the theoretical column flexural strength evaluated according to Eurocode 2 (EC2 2004). The lateral displacements at the column tip were recorded as  $\Delta_1$  and  $\Delta_2$  respectively, where the nominal yield displacement  $\Delta_y$  was determined by Eq. (2)

$$\Delta_y = \frac{4}{3} \left( \frac{\Delta_1 + |\Delta_2|}{2} \right) \quad (2)$$

The subsequent cycles are displacement-controlled. In the second cycle, the lateral displacement at the column tip were increased to  $+\Delta_y$  and  $-\Delta_y$  to reach  $\mu = +1$  and  $-1$  respectively, where  $\mu$  is the nominal displacement ductility factor defined as

$$\mu = \Delta / \Delta_y \quad (3)$$

In Eq. (3),  $\Delta$  = measured lateral displacement at the column tip. Starting from the third cycle when  $\mu = 2$ , the column was subjected to two full cycles. At the completion of every two cycles,  $\mu$  was increased by one provided that the strength degradation was not too excessive. The process is repeated until the measured moment capacity was smaller than 80% of the maximum measured flexural capacity.

### 2.4 Test observations

No flexural crack was observed in the first load-controlled elastic cycle for all specimens. The first flexural cracks occurred on the extreme tension fibres during the second cycle to reach  $\mu = \pm 1$ . This is because all tested specimens were subjected to very high axial load level and hence compressive stress. The subsequent development of flexural tension cracks needed to overcome this initial compressive stress at large lateral displacement. Similarly, the spalling of concrete cover on both extreme fibres was initiated by the compression crushes that occurred when the lateral displacement at the column tip was about to reach  $\mu = \pm 2$ . As the lateral displacement increased in succeeding inelastic cycles, the concrete cover continued to spall so that finally the longitudinal steel buckled owing to the loss of concrete cover.

## 3. Discussions of test results

### 3.1 Moment - displacement and moment - curvature hysteresis curves

Figs. 5 and 6 show the moment-displacement and moment-curvature hysteresis curves for all tested specimens. The first visible sign of concrete cover spalling and buckling of longitudinal steel have been marked on the moment-displacement curves. The value of theoretical moment  $M_u$  (as per Eurocode 2) is shown as a solid horizontal straight line, where the drop between this line and the dotted line indicates the secondary moment induced by  $P$ - $\Delta$  effect. In Fig. 5, the scales of nominal displacement ductility factor  $\mu$  and actual displacement ductility factor  $\mu'$  are shown. The actual displacement ductility factor is obtained by

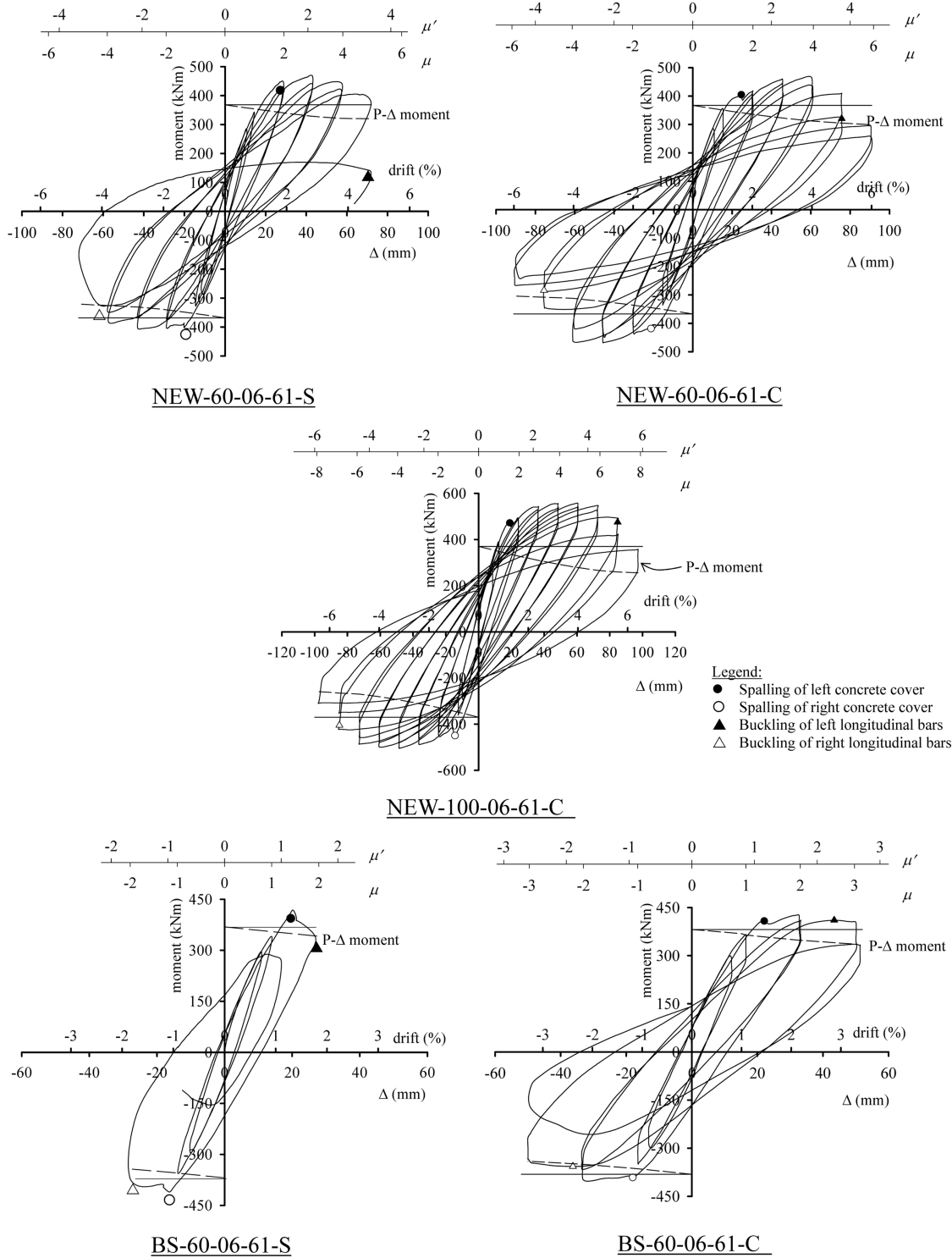


Fig. 5 Moment-displacement hysteresis curve of test specimens

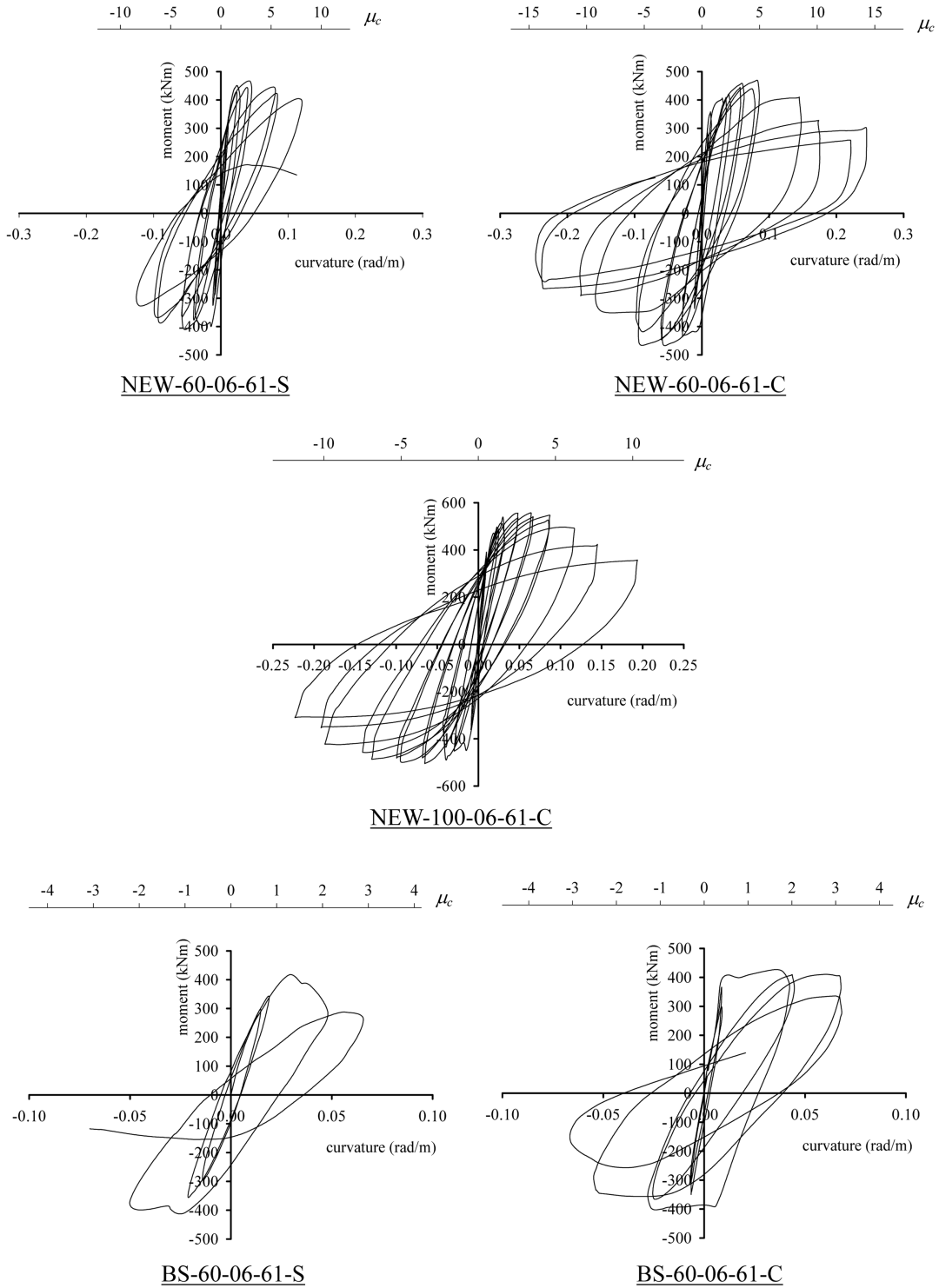


Fig. 6 Moment-curvature hysteresis curve of test specimens

Table 2 Comparison of theoretical and measured flexural strengths

Unit code	$P$ (kN) at $M_p$	$\rho_s$ (%)	$M_u$ (kNm)	$M_p$ (kNm)	$M_p/M_u$
NEW-60-06-61-S	3,270	2.10	344.0	466.4	1.36
NEW-60-06-61-C	3,232	2.00	367.1	469.0	1.28
NEW-100-06-61-C	5,348	3.20	369.7	557.5	1.51
BS-60-06-61-S	3,641	0.38	376.8	417.7	1.11
BS-60-06-61-C	3,635	0.47	393.9	426.7	1.08

Notes:  $M_u$  = Theoretical column flexural strength evaluated according to Eurocode 2  
 $M_p$  = Measured column flexural strength in experiment

$$\mu' = \Delta / \Delta'_y \tag{4}$$

$$\Delta'_y = \frac{4}{3} \left( \frac{\Delta'_1 + |\Delta'_2|}{2} \right) \tag{5}$$

where  $\Delta'_1$  and  $\Delta'_2$  are the lateral displacement of column measured at  $0.75M_p$  and  $-0.75M_p$  respectively, and  $M_p$  is the maximum measured moment capacity.

The following could be observed from Figs. 5 and 6:

- (1) The flexural strength of NEW specimens was attained within the inelastic cycle on the way to reach  $\mu = \pm 3$  or  $\pm 4$ . The occurrence of the maximum moment capacity beyond the elastic range is due to the confinement effect provided by the confining steel (Pam and Ho 2001). However, the flexural strength of BS specimens was reached in the cycle of  $\mu = \pm 2$  due to premature concrete core damage.
- (2) The increased content of confining steel and its 45° end hooks within the critical regions, which is manifested in the NEW specimens, effectively delayed the inelastic buckling of longitudinal steel as a result of very little hook deformation. Thus, it enabled the NEW specimens to withstand more inelastic cycles before the moment capacity dropped to less than 80% of the maximum flexural strength. This can be seen by comparing the performance of NEW-60-06-61-S with BS-60-06-61-S and that of NEW-60-06-61-C with BS-60-06-61-C.
- (3) The flexural strength enhancement ratio, which is defined by  $M_p/M_u$ , increases as the confining steel increases. The largest ratio of  $M_p/M_u$  (1.51) was attained by NEW-100-06-61-C. Table 2 summarises the  $M_p/M_u$  ratio for all specimens.

### 3.2 Ultimate displacement and curvature ductility factors

Displacement ductility and curvature ductility factors are commonly adopted to determine the flexural ductility of concrete columns (Park and Paulay 1975, Watson and Park 1994). The displacement ductility factor measures the ductility of the entire member as a function of section geometry, material strengths and plastic hinge length. The analytical evaluation of plastic hinge length has not been well established due to the complicated inelastic curvature profile within the plastic hinge region. Therefore, the displacement ductility factor is best obtained experimentally by destructive test. However, the curvature ductility factor  $\mu_c$  represents the section ductility, which could be obtained easily using nonlinear moment-curvature analysis based on the stress-strain curves of the constitutive materials and incorporates the strain history effect of longitudinal reinforcement

Table 3 Ultimate displacement and curvature ductility factors

Unit code	Average $P/A_g f'_c$	$\rho_s$ (%)	$\Delta'_y$ (mm)*	$\Delta_u$ (mm)	$\mu_d$	$\phi_y$ (rad/m)*	$\phi_u$ (rad/m)	$\mu_c$
NEW-60-06-61-S	0.61	2.10	20.4	68.6	3.4	0.0149	0.1230	8.3
NEW-60-06-61-C	0.59	2.00	20.0	79.9	4.0	0.0171	0.1742	10.2
NEW-100-06-61-C	0.64	3.20	19.9	89.7	4.5	0.0188	0.1944	10.4
BS-60-06-61-S	0.60	0.38	16.8	30.5	1.8	0.0228	0.0529	2.3
BS-60-06-61-C	0.60	0.47	19.1	38.9	2.0	0.0218	0.0522	2.4

\*Average absolute value obtained from positive and negative cycles

(Pam *et al.* 2001, Ho *et al.* 2003).

In this study, in order to take into account the flexural strength enhancement due to improved confinement effect provided by the confining steel, the actual displacement ductility factor  $\mu'$  (see Eq. (4)) is adopted instead of  $\mu$ . The member ductility capacity of the column, which is the displacement ductility at the ultimate state, is defined by the ultimate displacement ductility factor  $\mu_d$  as given by Eq. (6). The section ductility capacity of the column, which is the curvature ductility of the column at ultimate state, is defined in Eq. (7) by the ultimate curvature ductility factor  $\mu_c$ .

$$\mu_d = \Delta_u / \Delta'_y \quad (6)$$

$$\mu_c = \phi_u / \phi_y \quad (7)$$

$$\phi_y = \phi'_y / 0.75 \quad (8)$$

where  $\phi'_y$  is the measured curvature at  $0.75M_p$ ,  $\Delta_u$  and  $\phi_u$  are the respective displacement and curvature measured at  $0.8M_p$  in the post-peak range. The values of  $\mu_d$  and  $\mu_c$ , together with their corresponding yield values, are listed in Table 3. From Table 3, it is evident that the ultimate curvature ductility factors for all NEW specimens are significantly larger than those of BS specimens. This is due to the improved amount of confining steel provided in the column critical region. Moreover, the curvature ductility of the NEW specimens, whose confining steel was designed as per the proposed equation (Eq. (1)), were close to 10. The value is close to the normally assumed value for limited ductility structures (Watson *et al.* 1994). Such design would be most suitable for buildings located in low to medium risk seismic areas or in structures that prohibit the development of fully ductile response (e.g., closely spaced tall buildings).

### 3.3 Plastic hinge region and critical region

Plastic hinge region, which usually forms in the proximity of the section having maximum bending moment, indicates the extensive damage region when the structural member is subjected to reversed cyclic (or monotonic) displacement extended well into post-elastic range due to seismic attack, impact or overloading. Because there is significant inelastic damage within the plastic hinge region, substantial confining steel should be installed to protect the concrete core from premature crushing. Rigorously speaking, the plastic hinge length should be determined based on the actual

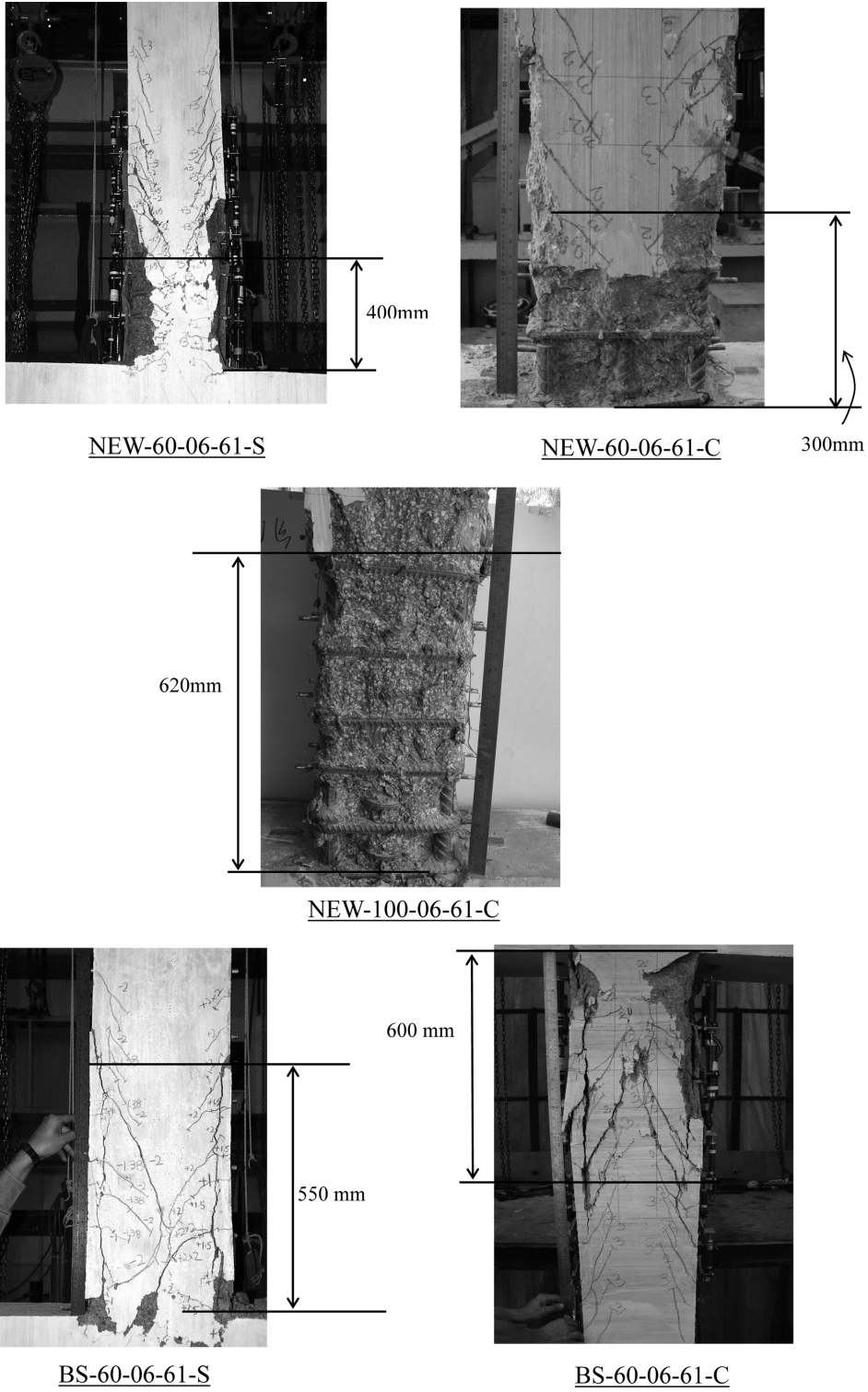


Fig. 7 Observed critical region of test specimens

column curvature profile including the effect of inelastic damage such that it matches with the rotation capacity and column drift at ultimate state. In this way, the determination of plastic hinge length requires the carrying out of destructive test of trial specimens, which may not be practicable in real design practice.

To handle the problem, the column region that suffered extensive inelastic damage including extensive concrete cover spalling, buckling of longitudinal steel, yielding of transverse steel and damage penetration into the concrete core, is identified as the critical region in this study. The critical region is not the same as the plastic hinge length, but however can provide an approximate column region for structural engineer to provide more confining steel without the need of carrying out destructive tests. In this study, two methods are proposed to determine the critical region, which are by physical observation of the extensively damaged regions of the failed columns and by determining the columns region with measured curvature larger than the yield curvature  $\phi_y$  (see Eq. (8)).

The first method is to observe the region of column suffering severe inelastic damage after failure. Fig. 7 shows the photos of all test specimens after failure and their identified critical region. It can be observed from the figure that the critical region of the BS specimens is larger than that of the counterpart NEW specimens. This is because the rotation capacities of BS specimens are very low owing to the small amount of confining steel provided. Hence, the damaged regions were forced to extend along the column height for longer length to develop large inelastic deflection at failure. On the contrary, the rotation capacities of the NEW specimens improved due to the larger amount of confining steel. Hence, the damaged region is relatively short comparing with the BS specimens under the same inelastic deflection. The average observed length of critical region (and those on the left and right hand sides of the column) from the beam-column interface is summarised in Table 4. Evidently, the observed length of critical region for all columns subjected to high axial load level: (1) is between  $0.9h$  and  $1.8h$ , where  $h$  is the column height; (2) increases as the amount of confining steel decreases or concrete strength increases.

The extent of critical region can also be determined from the curvature profile measured along the height of the column at ultimate state. The curvature profiles for all test specimens at ultimate state are plotted in Fig 8, where the horizontal axis shows the column curvature and the vertical axis shows the distance from the beam-column interface along column height. The curvature ductility factor at ultimate state is denoted by  $\mu_{us}$ , which has been indicated in each of the graphs in Fig. 8. The curvatures  $\phi$  in the columns are calculated based on the difference of the strain values between each pair of LVDTs located respectively at the extreme compression and tension faces of the column (Fig. 4), divided by their horizontal distance.

The values of  $\pm\phi_y$  obtained from Eq. (8) for the test specimens are plotted in Fig. 8 as vertical dashed lines. The length of critical region can then be identified as the region below the intersections of these two vertical lines and the curvature profiles, because it was observed that the column curvature increases dramatically after reaching  $\pm\phi_y$  owing to the extensive inelastic damage. The critical regions determined using this method are also listed in Table 4. It is obvious from the table that the critical region evaluated using the curvature profile are similar to those obtained by visual observation but none of the magnitude exceeds  $1.7h$ . By combining the results obtained from both methods, it is therefore proposed in this study that the length of critical regions for high-axially loaded HSC columns to be  $1.8h$ . The predetermined critical region length of  $2.0h$  for the test specimens is verified to be adequate.

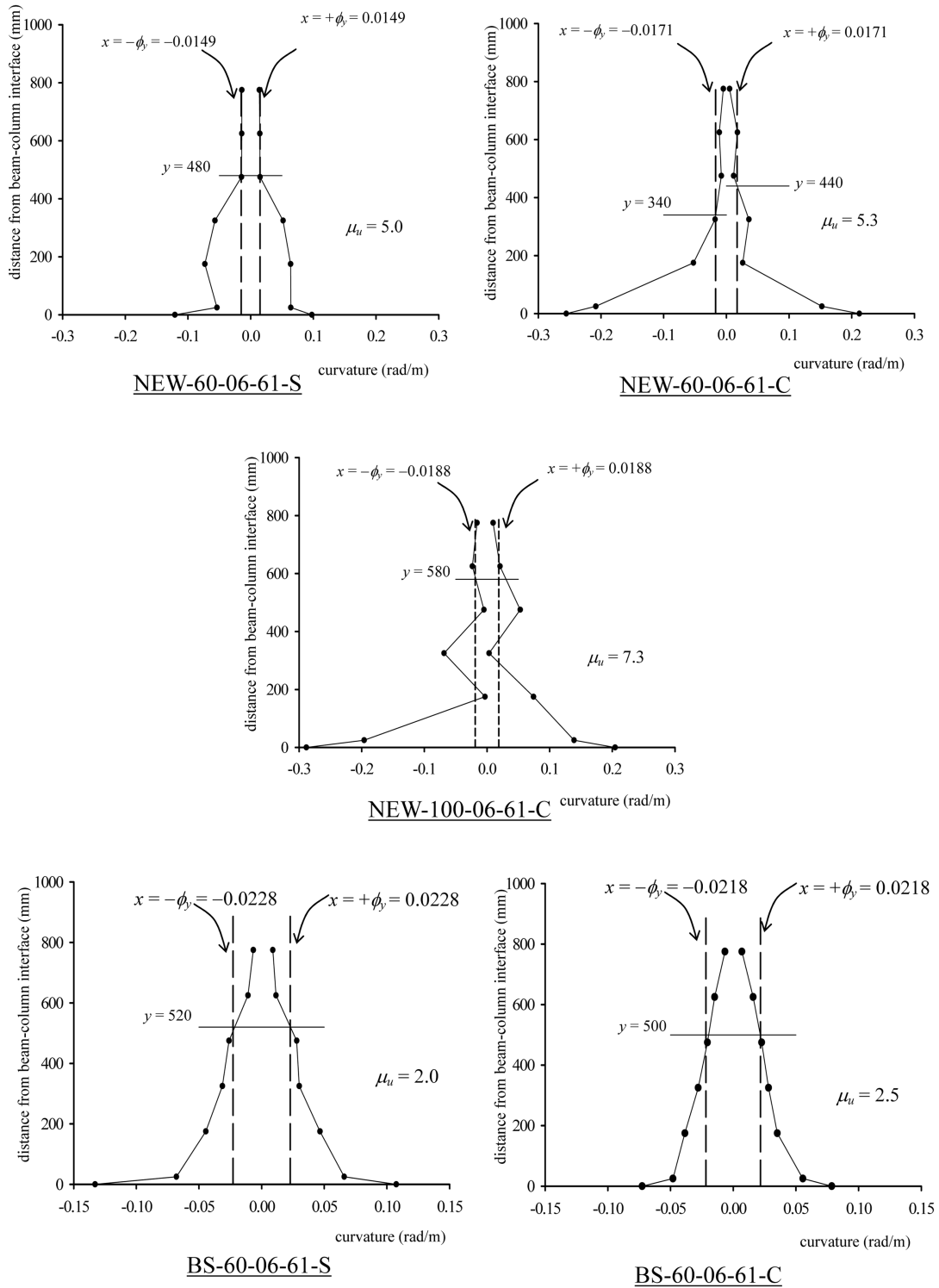


Fig. 8 Critical region length determined from measured curvature profiles

Table 4 Critical region length

Unit code	Average $P/A_g f'_c$	$\rho_s$ (%)	Average Observed critical region length (Left / Right)	Critical region length estimated using $\phi_y$ (+ve / -ve)
NEW-60-06-61-S	0.61	2.10	400 (400/400)	480 (480/480)
NEW-60-06-61-C	0.59	2.00	300 (300/300)	390 (340/440)
NEW-100-06-61-C	0.64	3.20	620 (620/620)	580 (580/580)
BS-60-06-61-S	0.60	0.38	550 (550/550)	520 (520/520)
BS-60-06-61-C	0.60	0.47	600 (600/600)	500 (500/500)

Note: All critical region length expressed in mm.

#### 4. Proposed design guidelines for high-axially loaded HSC columns

Based on the experimental results obtained in this study, the following guidelines are proposed for designing limited ductility HSC columns subjected to high compressive axial load level ( $P/A_g f'_c = 0.6$ ):

- (1) The content of confining steel within the critical region of columns should be designed using Eq. (1), whereas that outside the critical region can be designed as per the ultimate shear resistance.
- (2) The length of critical region, in which the amount of confining steel designed as per Eq. (1) should be installed, should not be less than  $1.8h$  ( $h$  is the column height).
- (3)  $45^\circ$  end hooks in confining steel should be provided within the critical region while  $90^\circ$  end hooks can be used elsewhere.

#### 5. Conclusions

Five high-strength concrete (HSC) columns subjected to large compressive axial load level ( $P/A_g f'_c = 0.6$ ) and containing confining steel designed either based on author's proposed design equation (NEW specimens) or the ultimate shear demand (BS specimens) were tested under large reversed cyclic inelastic displacement excursions. From the test results, it is concluded that for high-axially loaded HSC columns:

- (1) The flexural strength occurred within inelastic range at  $\mu \geq 3$ .
- (2) Confining steel designed according to solely the ultimate shear demand would have low ultimate displacement and curvature ductility factors. The design may not provide adequate ductility to columns in low to moderate seismicity regions.
- (3) The critical region length of HSC columns subjected to high axial load level can be determined either by physical observation or by identifying the column region with measured curvature larger than yield curvature  $\phi_y$ . The critical regions determined by both methods agree well with each other. For design purpose, the critical region length of HSC columns subjected to high axial load level can be taken as not less than  $1.8h$ .
- (4) The  $90^\circ$  end hooks of confining steel were pushed open by the buckled longitudinal steel within the critical region while the  $45^\circ$  end hooks were effective in restraining the longitudinal

steel without hook deformation. Therefore, 45° end hooks should be used within critical region.

- (5) The confining steel calculated based on the authors' proposed equation improved considerably the column curvature ductility factor to about 10, which is considered adequate for designing high-axially loaded limited ductility HSC columns located in low to moderate seismicity areas.

## Acknowledgements

Generous support from Seed Funding Programme for Basic Research (Project number 200802159007) provided by The University of Hong Kong (HKU) is gratefully acknowledged. The author would also like to thank the laboratory staff of the Department of Civil Engineering, HKU, for their technical support provided in the experimental tests.

## References

- Ates, S., Soyuluk, K., Dumanoglu, A.A. and Bayraktar, A. (2009), "Earthquake response of isolated cable-stayed bridges under spatially varying ground motions", *Struct. Eng. Mech.*, **31**(6), 639-662.
- Altin, S., Kuran, F., Anil, O. and Kara, M.E. (2008), "Rehabilitation of heavily earthquake damaged masonry building using steel straps", *Struct. Eng. Mech.*, **30**(6), 651-664.
- Bae, S. and Bayrak, O. (2008), "Plastic hinge length of reinforced concrete columns", *ACI Struct. J.*, **105**(3), 290-300.
- Bambach, M.R., Jama, H., Zhao, X.L. and Grzebieta, R.H. (2008), "Hollow and concrete filled steel hollow sections under transverse impact loads", *Eng. Struct.*, **30**, 2859-2870.
- Bayrak, O. and Sheikh, S.A. (1998), "Confinement reinforcement design considerations for ductile HSC columns", *J. Struct. Eng.-ASCE*, **124**(9), 999-1010.
- Bechtoula, H., Kono, S. and Watanabe, F. (2009), "Seismic performance of high strength reinforced concrete columns", *Struct. Eng. Mech.*, **31**(6), 697-716.
- Bindhu, K.R., Jaya, K.P. and Manicka Selvam, V.K. (2008), "Seismic resistance of exterior beam-column joints with non-conventional confinement reinforcement detailing", *Struct. Eng. Mech.*, **30**(6), 733-761.
- Chen, Y.H. and Ding, Y.J. (2008), "Passive, semi-active, and active tuned-liquid-column dampers", *Struct. Eng. Mech.*, **30**(1), 1-20.
- Chen, S., Jia, Y. and Wang, X. (2009), "Experimental study of moment redistribution and load carrying capacity of externally prestressed continuous composite beams", *Struct. Eng. Mech.*, **31**(5), 615-619.
- Chung, T.S.K., Lam, E.S.S., Wu, B. and Xu, Y.L. (2009), "Experimental and numerical verification of hydraulic displacement amplification damping system", *Struct. Eng. Mech.*, **33**(1), 1-14.
- EC2, Eurocode 2 (2004), *Eurocode 2: Design of Concrete Structures: Part 1-1: General Rules and Rules for Buildings*, UK.
- Elmenschawi, A. and Brown, T. (2011) "Modelling criteria for R/C elements constructed with ultra-high-strength concrete and subjected to cyclic loading", *Struct. Des. Tall Spec.*, **20**(3), 371-386.
- Elremaily, A. and Azizinamini, A. (2002), "Behavior and strength of circular concrete-filled tube columns", *J. Constr. Steel Res.*, **58**(12), 1567-1591.
- Ellobody, E. and Young, B. (2006), "Design and behaviour of concrete-filled cold-formed stainless steel tube columns", *Eng. Struct.*, **28**, 716-728.
- Englekirk, R.E. (2008), "A call for change in seismic design procedures", *Struct. Des. Tall Spec.*, **17**, 1005-1013.
- Feng, R. and Young, B. (2009) "Behaviour of concrete-filled stainless steel tubular X-joints subjected to compression", *Thin Wall. Struct.*, **47**(4), 365-374.
- Fu, C. (2009), "Passive vibration control of plan-asymmetric buildings using tuned liquid column gas dampers",

- Struct. Eng. Mech.*, **33**(3), 339-355.
- Ghosh, R.K. and Ghosh, A.D. (2008), "Soil interaction effects on the performance of compliant liquid column damper for seismic vibration control of short period structures", *Struct. Eng. Mech.*, **28**(1), 89-105.
- Hashemi, S.H., Maghsoudi, A.A. and Rahgozar, R. (2008), "Flexural ductility of reinforced HSC beams strengthened CFRP sheets", *Struct. Eng. Mech.*, **30**(4), 403-426.
- Hino, J., Yoshitomi, S., Tsuji, M. and Takewaki, I. (2008), "Bound of aspect ratio of base-isolated buildings considering nonlinear tensile behavior of rubber bearing", *Struct. Eng. Mech.*, **30**(3), 351-368.
- Ho, J.C.M. and Pam, H.J. (2003a), "Influence of transverse steel configuration on post-elastic behaviour of high-strength reinforced concrete columns", *Trans. Hong Kong Institut. Eng.*, **10**(2), 1-9.
- Ho, J.C.M. and Pam, H.J. (2003b), "Inelastic design of low-axially loaded high-strength reinforced concrete columns", *Eng. Struct.*, **25**(8), 1083-1096.
- Ho, J.C.M., Kwan, A.K.H. and Pam, H.J. (2003), "Theoretical analysis of post-peak flexural behaviour of normal- and high-strength concrete beams", *Struct. Des. Tall Spec.*, **12**, 109-125.
- Ho, J.C.M. (2011), "Limited ductility design of reinforced concrete columns for tall buildings in low to moderate seismicity regions", *Struct. Des. Tall Spec.*, **20**, 102-120.
- Ho, J.C.M., Lam, J.Y.K. and Kwan, A.K.H. (2010), "Effectiveness of adding confinement for ductility improvement of high-strength concrete columns", *Eng. Struct.*, **32**, 714-725.
- Inel, M., Ozmen, H.B. and Bilgin, H. (2008), "Seismic performance evaluation of school buildings in Turkey", *Struct. Eng. Mech.*, **30**(5), 535-558.
- Kaklauskas, G., Gribniak, V., Bacinskas, D. and Vainiūnas, P. (2009), "Shrinkage influence on tension stiffening in concrete members", *Eng. Struct.*, **31**(6), 1305-1312.
- Kavianipour, O. and Sadati, S.H. (2009), "Effects of damping on the linear stability of a free-free beam subjected to follower and transversal forces", *Struct. Eng. Mech.*, **33**(6), 709-724.
- Kim, T.H., Kim, Y.J. and Shin, H.M. (2008a), "Seismic performance assessment of reinforced concrete bridge piers supported by laminated rubber bearings", *Struct. Eng. Mech.*, **29**(3), 259-278.
- Kim, D., Yi, J.H., Seo, H.Y. and Chang, C. (2008b), "Earthquake risk assessment of seismically isolated extradosed bridges with lead rubber bearings", *Struct. Eng. Mech.*, **29**(6), 689-707.
- Kwan, A.K.H. (2000), "Use of condensed silica fume for making high-strength, self-consolidating concrete", *Can. J. Civil Eng.*, **27**(4), 620-627.
- Lam, J.Y.K., Ho, J.C.M. and Kwan, A.K.H. (2009a), "Flexural ductility of high-strength concrete columns with minimal confinement", *Mater. Struct.*, **42**(7), 909-921.
- Lam, J.Y.K., Ho, J.C.M. and Kwan, A.K.H. (2009b), "Maximum axial load level and minimum confinement for limited ductility design of concrete columns", *Comput. Concrete*, **6**(5), 357-376.
- Lew, M. (2007), "Design of tall buildings in high-seismic regions", *Struct. Des. Tall Spec.*, **16**, 537-541.
- Li, B., Park, R. and Tanaka, H. (1991), "Effect of confinement on the behaviour of high strength concrete columns under seismic loading", *Proceedings, Pacific Conference on Earthquake Engineering*, Auckland, November.
- Li, C. and Xiong, X. (2008), "Estimation of active multiple tuned mass dampers for asymmetric structures", *Struct. Eng. Mech.*, **29**(5), 505-530.
- Logan, A., Choi, W., Mirmiran, A., Rizkalla, S. and Zia, P. (2009), "Short-term mechanical properties of high-strength concrete", *ACI Mater. J.*, **106**(5), 413-418.
- Lu, X. and Hsu, C.T.T. (2007), "Tangent Poisson's ratio of high-strength concrete in triaxial compression", *Mag. Concrete Res.*, **59**(1), 69-77.
- Lu, X. and Zhou, Y. (2007), "An applied model for steel reinforced concrete columns", *Struct. Eng. Mech.*, **27**(6), 697-711.
- Maghsoudi, A.A. and Bengar, H.A. (2006), "Flexural ductility of HSC members", *Struct. Eng. Mech.*, **24**(2), 195-212.
- Mirmiran, A. and Shahawy, M. (1997), "Dilation characteristics of confined concrete", *Mech. Cohes. Frict. Mater.*, **2**, 237-249.
- Pam, H.J. and Ho, J.C.M. (2001), "Flexural strength enhancement of confined reinforced concrete columns", *Proceedings, Institution of Civil Engineers, Structures and Buildings*, **146**(4), 363-370.
- Pam, H.J., Kwan, A.K.H. and Ho, J.C.M. (2001), "Post-peak behavior and flexural ductility of doubly reinforced

- normal- and high-strength concrete beams”, *Struct. Eng. Mech.*, **12**(5), 459-474.
- Pam, H.J. and Ho, J.C.M. (2009), “Length of critical region for confinement steel in limited ductility high-strength reinforced concrete columns”, *Eng. Struct.*, **31**, 2896-2908.
- Park, R. and Paulay, T. (1975), *Reinforced Concrete Structures*, John Wiley & Sons, New York, USA.
- Park, R. (1982), “Ductility of square-confined concrete columns”, *J. Struct. Eng.-ASCE*, **108ST**(2), 929-950.
- Park, R. (2001), “Improving the resistance of structures to earthquakes”, *B. N.Z. Nat. Soc. Earthq. E.*, **34**(1), 1-39.
- Paultre, P., Legeron, F. and Mongeau, D. (2001), “Influence of concrete strength and transverse reinforcement yield strength on behaviour of high-strength concrete columns”, *ACI Struct. J.*, **98**(4), 490-501.
- Sadjadi, R. and Kianoush, M.R. (2010), “Application of fiber element in the assessment of the cyclic loading behavior of RC columns”, *Struct. Eng. Mech.*, **34**(3), 301-317.
- Su, R.K.L., Lam, W.Y. and Pam, H.J. (2009) “Experimental study of plate-reinforced composite deep coupling beams”, *Struct. Des. Tall Spec.*, **18**, 235-257.
- Tsang, H.H., Su, R.K.L., Lam, N.T.K. and Lo, S.H. (2009), “Rapid assessment of seismic demand in existing building structures”, *Struct. Des. Tall Spec.*, **18**, 427-439.
- Watson, S. and Park, R. (1994), “Simulated seismic load tests on reinforced concrete columns”, *J. Struct. Eng.-ASCE*, **120**(6), 1825-1849.
- Watson, S., Zahn, F.A. and Park, R. (1994), “Confining reinforcement for concrete columns”, *J. Struct. Eng.-ASCE*, **120**(6), 1799-1824.
- Weerheijm, J., Mediavilla, J. and van Doormaal, J.C.A.M. (2009), “Explosive loading of multi storey RC buildings: Dynamic response and progressive collapse”, *Struct. Eng. Mech.*, **32**(2), 193-212.
- Wu, W.J. and Cai, C.S. (2009), “Comparison of deck-anchored damper and clipped tuned mass damper on cable vibration reduction”, *Struct. Eng. Mech.*, **32**(6), 741-754.
- Wu, Y.F., Oehlers, D.J. and Griffith, M.C. (2004), “Rational definition of the flexural deformation capacity of RC column sections”, *Eng. Struct.*, **26**, 641-650.
- Wu, Y.F. and Wei, Y.Y. (2010), “Effects of cross-sectional aspect ratio on the strength of CFRP-confined rectangular concrete columns”, *Eng. Struct.*, **32**, 32-45.
- Yagob, O., Galal, K. and Naumoski, N. (2009), “Progressive collapse of reinforced concrete structures”, *Struct. Eng. Mech.*, **32**(6), 771-786.
- Yan, Z.H. and Au, F.T.K. (2010), “Nonlinear dynamic analysis of frames with plastic hinges at arbitrary locations”, *Struct. Des. Tall Spec.*, **19**, 778-801.
- Zhang, G., Liu, B., Bai, G. and Liu, J. (2009), “Experimental study on seismic behavior of high strength reinforced concrete frame columns with high axial compression ratios”, *Struct. Eng. Mech.*, **33**(5), 653-656.
- Zhu, Y. and Su, R.K.L. (2010), “Seismic behavior of strengthened reinforced concrete coupling beams by bolted steel plates, Part 2: Evaluation of theoretical strength”, *Struct. Eng. Mech.*, **34**(5), 563-580.

**Notations**

$A_c$	: Core concrete area measured to outside of confining steel
$A_g$	: Gross area of column cross section
$d$	: Effective depth of column cross-section
$d_s$	: Diameter of confining steel
$f'_c$	: Concrete cylinder compressive strength
$f_y$	: Yield strength of longitudinal steel
$f_{ys}$	: Yield strength of confining steel
$h$	: Height of column cross-section
$M_p$	: Measured maximum moment capacity
$M_u$	: Flexural strength calculated using Eurocode 2
$P$	: Compressive axial load
$\Delta$	: Measured lateral displacement of column tip
$\Delta_u$	: Measured lateral displacement of column tip at $0.8M_p$ post-peak
$\Delta_y, \Delta'_y$	: Nominal and actual yield displacements
$\Delta_1, \Delta_2$	: Measured lateral displacement at $+0.75M_u$ and $-0.75M_u$ respectively
$\Delta'_1, \Delta'_2$	: Measured lateral displacement at $+0.75M_p$ and $-0.75M_p$ respectively
$\phi$	: Curvature in column
$\phi_u$	: Ultimate curvature at $0.8M_p$ post-peak
$\phi_y$	: Yield curvature
$\phi'_y$	: Measured column curvature at $0.75M_p$
$\mu, \mu'$	: Nominal and actual displacement ductility factors
$\mu_c$	: Ultimate curvature ductility factor
$\mu_d$	: Ultimate displacement ductility factor
$\rho$	: Area ratio of longitudinal steel
$\rho_s$	: Volumetric ratio of confining steel